

Triangle singularities in the $T_{cc}^+ \rightarrow D^{*+}D^0 \rightarrow \pi^+D^0D^0$ decay width

N.N. Achasov * and G.N. Shestakov †

Laboratory of Theoretical Physics, S.L. Sobolev Institute for Mathematics, 630090, Novosibirsk, Russia

The values of the masses of the particles involved in the decay of $T_{cc}^+ \rightarrow D^{*+}D^0 \rightarrow \pi^+D^0D^0$ suggest that due to the final state interactions in the transition vertex $T_{cc}^+ \rightarrow D^{*+}D^0$ there may be triangle logarithmic singularities. We discuss their possible role and show that the tree approximation for calculating the decay widths $T_{cc}^+ \rightarrow (D^{*+}D^0 + D^{*0}D^+) \rightarrow \pi^+D^0D^0, \pi^0D^0D^+, \gamma D^0D^+$ is quite sufficient at the current level of measurement accuracy.

I. INTRODUCTION

At the end of July 2021, the LHCb Collaboration announced the discovery of the doubly charmed tetraquark T_{cc}^+ [1, 2] and then published detailed measurement results along with their theoretical processing and interpretation [3, 4]. Over the next days, weeks and months, a very interesting discussion is going on in the literature about the possible internal structure of the T_{cc}^+ state, about the mechanisms of its production and decay through intermediate states $D^{*+}D^0$ and $D^{*0}D^+$, on the possible values of its total decay width and partial decay widths into coupled channels $\pi^+D^0D^0, \pi^0D^0D^+$, and γD^0D^+ , about its line shape and the shapes of the two-particle mass spectra DD and πD , as well as about the possible existence of other similar states. A detailed discussion of all these issues can be found in [5–17]; see also the references cited therein.

In Sec. II of this article, we discuss the possible role of triangle singularities in the width of the decay $T_{cc}^+[3.875; I(J^P) = 0(1^+)] \rightarrow D^{*+}(J^P = 1^-)D^0(J^P = 0^-) \rightarrow \pi^+D^0D^0$. In so doing, we proceed within the framework of a scalar model, i.e., we treat all particles in this decay as spinless and scalar. Such a simplification, however, seems quite reasonable. First, the decay of $T_{cc}^+ \rightarrow D^{*+}D^0$ occurs in the near-threshold region and therefore is mainly S wave. Second, the ratio of the $D^{*+} \rightarrow (D\pi)^+$ decay width (it is ≈ 83 keV [18]) to the distance to the $(D\pi)^+$ threshold is $\approx 1/70$ and, consequently, the change of this width on the energy interval of the order of itself is small (i.e., in the $D^{*+}(2010)$ region, it is almost constant). The formulas [see below Eqs. (3) and (4)], which we use to estimate the possible role of interactions of D^*D pairs in the final state, are in fact expansions of the Omnès functions (solutions) for form factors [19] in case of weak coupling (i.e., smallness of D^*D scattering at low energies). Discussions of a number of dynamic approximations of the Omnès functions can be found, for example, in Refs. [20, 21]. The performed analysis allows us to conclude that the tree approximation used in Refs. [3, 4] for calculating the decay widths $T_{cc}^+ \rightarrow (D^{*+}D^0 + D^{*0}D^+) \rightarrow \pi^+D^0D^0, \pi^0D^0D^+, \gamma D^0D^+$ is quite sufficient at the current level of measurement accuracy.

The LHCb Collaboration results [3, 4] obtained from the fit to the $\pi^+D^0D^0$ mass spectrum indicates that the Breit-Wigner mass of the T_{cc}^+ relative to the $D^{*+}D^0$ mass threshold $\delta m_{BW} = -273 \pm 61$ keV and its Breit-Wigner width $\Gamma_{BW} = 410 \pm 165$ keV (only statistical uncertainties are indicated here). The measured δm_{BW} value corresponds to a mass of approximately 3875 MeV.

II. $T_{cc}^+ \rightarrow D^{*+}D^0 \rightarrow \pi^+D^0D^0$ DECAY IN THE SCALAR MODEL

In the tree approximation, the $T_{cc}^+ \rightarrow D^{*+}D^0 \rightarrow \pi^+D^0D^0$ decay is described by two diagrams shown in Fig. 1 which differ in the permutation of identical D^0 mesons. The corresponding decay width is given by

$$\Gamma_{T_{cc}^+ \rightarrow D^{*+}D^0 \rightarrow \pi^+D^0D^0}(s_1) = \frac{g_{T_{cc}^+D^{*+}D^0}^2}{16\pi} \frac{g_{D^{*+}\pi^+D^0}^2}{16\pi} \frac{1}{2\pi s_1^{3/2}} \int_{(m_{D^0} + m_{\pi^+})^2}^{(\sqrt{s_1} - m_{D^0})^2} ds \int_{t_-(s_1, s)}^{t_+(s_1, s)} dt \left| \frac{1}{D(s)} + \frac{1}{D(t)} \right|^2, \quad (1)$$

where s_1 is the invariant mass squared of the virtual T_{cc}^+ state, s and t are the $\pi^+D_{(1)}^0$ and $\pi^+D_{(2)}^0$ invariant mass squared, respectively, and $t_{\pm}(s_1, s)$ denote the boundaries of the physical region for the variable t for fixed values

* achasov@math.nsc.ru

† shestako@math.nsc.ru

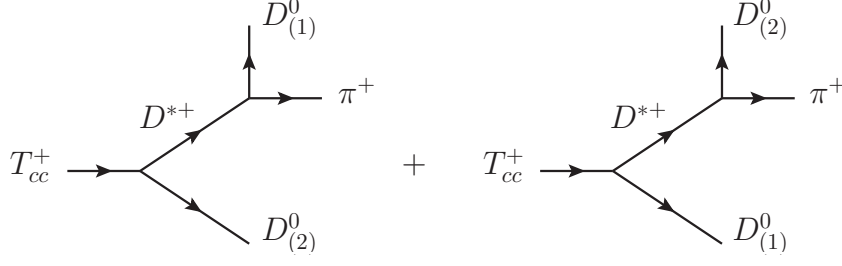


Figure 1: The tree diagrams for the decay $T_{cc}^+ \rightarrow D^{*+} D^0 \rightarrow \pi^+ D^0 D^0$.

of s_1 and s [22]; $g_{T_{cc}^+ D^{*+} D^0}$ and $g_{D^{*+} \pi^+ D^0}$ are the effective coupling constants. The inverse propagator of the D^{*+} resonance, $D(s)$, has the form

$$D(s) = m_{D^{*+}}^2 - s - i\sqrt{s}\Gamma_{D^{*+}}^{tot}(s) = m_{D^{*+}}^2 - s - i\frac{g_{D^{*+}\pi^+D^0}^2}{16\pi} \left[\rho_{\pi^+ D^0}(s) + \frac{1}{2} \rho_{\pi^0 D^+}(s) \right], \quad (2)$$

where $\rho_{\pi D}(s) = \sqrt{s^2 - 2s(m_\pi^2 + m_D^2) + (m_\pi^2 - m_D^2)^2}/s$; factor 1/2 at $\rho_{\pi^0 D^+}(s)$ follows from the isotopic symmetry. We neglect the contribution of the $D^{*+} \rightarrow D^+ \gamma$ decay, which is $\approx 1.6\%$. From the Particle Data Group data [18] about $\Gamma_{D^{*+}}^{tot}(m_{D^{*+}}^2) = 83.4$ keV we find $g_{D^{*+}\pi^+D^0}^2/(16\pi) \approx 0.00289$ GeV². We also set $g_{T_{cc}^+ D^{*+} D^0}^2/(16\pi) = 0.5$ GeV² for definiteness. A comprehensive discussion of possible values of this constant which it can be extracted from the fit of the T_{cc}^+ line shape is presented in Ref. [4]. Let us note that the relative magnitude of the effect that we consider here does not depend on the value of the constant $g_{T_{cc}^+ D^{*+} D^0}$. The energy dependent width $\Gamma_{T_{cc}^+ \rightarrow D^{*+} D^0 \rightarrow \pi^+ D^0 D^0}(s_1)$ calculated in the tree approximation using Eqs. (1) and (2) is shown in Fig. 2. Note that for large values of $g_{T_{cc}^+ D^{*+} D^0}$ the sharp increase of $\Gamma_{T_{cc}^+ \rightarrow D^{*+} D^0 \rightarrow \pi^+ D^0 D^0}(s_1)$ and $\Gamma_{T_{cc}^+ \rightarrow (D^{*+} D^0 + D^{*0} D^+) \rightarrow \pi^0 D^0 D^+}(s_1)$ above the $D^* D$ thresholds and a similar growth of the real part of the self-energy function under the $D^* D$ thresholds in the T_{cc}^+ propagator lead to a sharp suppression of the right and left wings of the T_{cc}^+ resonance peak. A similar phenomenon takes place for the four-quark $a_0(980)$ resonance [23].

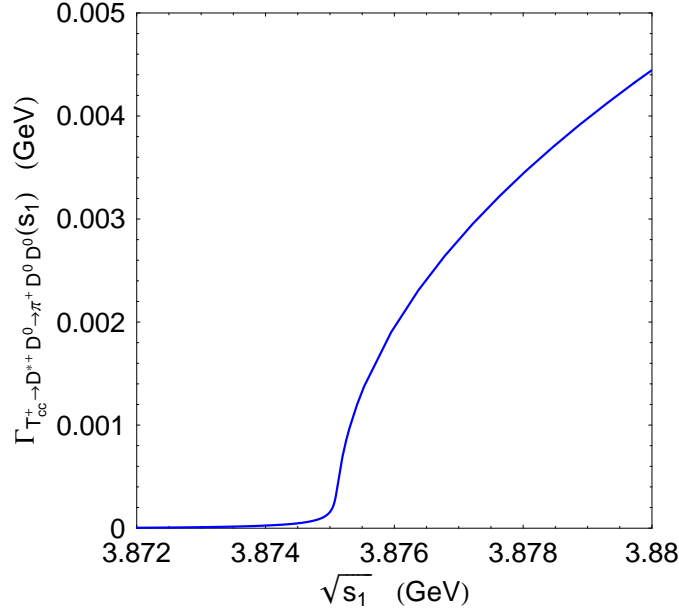


Figure 2: The $T_{cc}^+ \rightarrow D^{*+} D^0 \rightarrow \pi^+ D^0 D^0$ decay width as a function of $\sqrt{s_1}$ calculated by Eqs. (1) and (2).

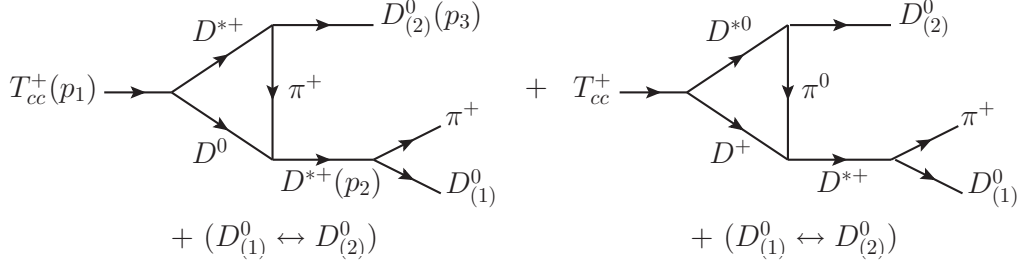


Figure 3: The simplest diagrams that take into account final state interactions in the $T_{cc}^+ \rightarrow D^{*+} D^0 \rightarrow \pi^+ D^0 D^0$ decay.

The values of the masses of the particles involved in the decay of $T_{cc}^+ \rightarrow D^{*+} D^0 \rightarrow \pi^+ D^0 D^0$ suggest that due to the final state interactions in the vertex transition $T_{cc}^+ \rightarrow D^{*+} D^0$ there may be triangle logarithmic singularities. Examples of corresponding ‘‘dangerous’’ diagrams are shown in Fig. 3. Take into account their contribution to the decay width $\Gamma_{T_{cc}^+ \rightarrow D^{*+} D^0 \rightarrow \pi^+ D^0 D^0}(s_1)$ can be done by the following substitutions in Eq. (1):

$$\frac{1}{D(s)} \rightarrow \frac{1}{D(s)} \left[1 + \frac{g_{D^{*+}\pi^+D^0}^2}{16\pi} \left(F_{D^{*+}D^0}(s_1, s) + \frac{1}{2} F_{D^{*0}D^+}(s_1, s) \right) \right], \quad (3)$$

$$\frac{1}{D(t)} \rightarrow \frac{1}{D(t)} \left[1 + \frac{g_{D^{*+}\pi^+D^0}^2}{16\pi} \left(F_{D^{*+}D^0}(s_1, t) + \frac{1}{2} F_{D^{*0}D^+}(s_1, t) \right) \right], \quad (4)$$

where $F_{D^{*+}D^0}$ and $F_{D^{*0}D^+}$ are the amplitudes of the triangle loops included in the diagrams in Fig. 3; the factor 1/2 at $F_{D^{*0}D^+}$ follows from isotopic symmetry. In our normalization

$$F_{D^{*+}D^0}(s_1, s) = \frac{i}{\pi^3} \int \frac{d^4k}{D_1 D_2 D_3}, \quad (5)$$

where $D_1 = k^2 - m_{D^{*+}}^2 + i\epsilon$, $D_2 = (p_1 - k)^2 - m_{D^0}^2 + i\epsilon$, and $D_3 = (k - p_3)^2 - m_{\pi^+}^2 + i\epsilon$ are the inverse propagators of the particles in the loop. Here and in Fig. 3 p_1, p_2, p_3 denote the 4-momenta of the particles in the reaction; $p_1 = p_2 + p_3$, $p_1^2 = s_1$, $p_2^2 = s$, and $p_3^2 = m_{D^0}^2$. The amplitude $F_{D^{*0}D^+}(s_1, s)$ has a similar form.

If the values of the variables \sqrt{s} and $\sqrt{s_1}$ are simultaneously in the intervals

$$m_1 + m_2 < \sqrt{s_1} < \sqrt{m_1^2 + m_2^2 + m_2 m_3 + (m_2/m_3)(m_1^2 - m_{D^0}^2)}, \quad (6)$$

$$m_2 + m_3 < \sqrt{s} < \sqrt{[(m_1 + m_2)(m_1 m_2 + m_3^2) - m_2 m_{D^0}^2]/m_1}, \quad (7)$$

where m_1, m_2 , and m_3 are the particle masses in the inverse propagators D_1, D_2 , and D_3 , respectively [see Eq. (5)], then for each value of s , there is a unique value s_1 (and vice versa) for which the imaginary part of the amplitude $F_{D^{*+}D^0}(s_1, s)$ [and similarly that of $F_{D^{*0}D^+}(s_1, s)$] has a logarithmic singularity (see, for example, Refs. [24–27] and references herein). Note that the minimum value of s_1 in (6) herewith corresponds to the maximum value of s in (7) (and vice versa). In the amplitude $F_{D^{*+}D^0}(s_1, s)$ (see the left diagram in Fig. 3) $m_1 = m_{D^{*+}}, m_2 = m_{D^0}, m_3 = m_{\pi^+}$ and for it the numerical values of the intervals in Eqs. (6) and (7) are as follows:

$$3.8751 \text{ GeV} < \sqrt{s_1} < 3.91259 \text{ GeV} \quad (0 < \sqrt{s_1} - (m_{D^{*+}} + m_{D^0}) < 37.49 \text{ MeV}), \quad (8)$$

$$2.00441 \text{ GeV} < \sqrt{s} < 2.00946 \text{ GeV} \quad (0 < \sqrt{s} - (m_{D^0} + m_{\pi^+}) < 5.05 \text{ MeV}). \quad (9)$$

Here in parentheses are the corresponding intervals in units of MeV into which the invariant masses $\sqrt{s_1}$ and \sqrt{s} with the subtracted threshold values should fall. In the amplitude $F_{D^{*0}D^+}(s_1, s)$ (see the right diagram in Fig. 3) $m_1 = m_{D^{*0}}, m_2 = m_{D^+}, m_3 = m_{\pi^0}$ and for it, respectively, we have

$$3.87651 \text{ GeV} < \sqrt{s_1} < 3.92318 \text{ GeV} \quad (0 < \sqrt{s_1} - (m_{D^{*0}} + m_{D^+}) < 46.67 \text{ MeV}), \quad (10)$$

$$2.00464 \text{ GeV} < \sqrt{s} < 2.01073 \text{ GeV} \quad (0 < \sqrt{s} - (m_{D^+} + m_{\pi^0}) < 6.05 \text{ MeV}). \quad (11)$$

Since $m_{D^{*+}} = 2.01026 \text{ GeV}$ is greater than $(\sqrt{s})_{max} = 2.00946 \text{ GeV}$ in Eq. (9), then due to the contribution of the amplitude $F_{D^{*+}D^0}(s_1, s \approx m_{D^{*+}}^2)$ in the vertex $T_{cc}^+ D^{*+} D^0$ no triangle singularity arises. At the same time, $m_{D^{*+}} =$

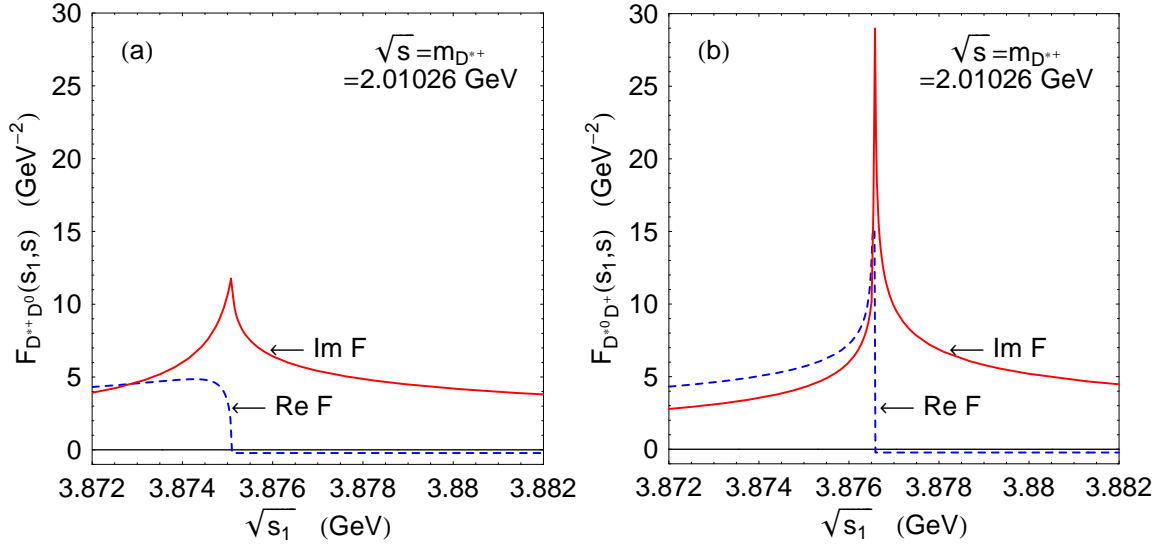


Figure 4: The solid and dashed curves show, respectively, imaginary and real parts of the amplitudes (a) $F_{D^{*+}D^0}(s_1, s)$ and (b) $F_{D^{*0}D^+}(s_1, s)$ for $\sqrt{s} = m_{D^{*+}}$. In the vicinity of the D^{*+} resonance (i.e., at $\sqrt{s} \approx m_{D^{*+}}$) the functions $F_{D^{*+}D^0}(s_1, s)$ and $F_{D^{*0}D^+}(s_1, s)$ have a similar behavior.

2.01026 GeV is less than $(\sqrt{s})_{max} = 2.01073$ GeV in Eq. (11) and therefore in the amplitude $F_{D^{*0}D^+}(s_1, s \approx m_{D^{*+}}^2)$ (and hence in the $T_{cc}^+ D^{*+} D^0$ vertex) the triangle singularity occurs at $\sqrt{s_1} \approx 3.87658$ GeV. Figure 4 shows the imaginary and real parts of the amplitudes $F_{D^{*+}D^0}(s_1, s = m_{D^{*+}}^2)$ and $F_{D^{*0}D^+}(s_1, s = m_{D^{*+}}^2)$ as functions of $\sqrt{s_1}$ calculated using the method developed in Refs. [28, 29]. As can be seen from this figure, the functions $F_{D^{*+}D^0}(s_1, s = m_{D^{*+}}^2)$ and $F_{D^{*0}D^+}(s_1, s = m_{D^{*+}}^2)$ are not small by themselves (one of them is even singular). However, in Eqs. (3) and (4), the contributions from $F_{D^{*+}D^0}(s_1, s)$ and $F_{D^{*0}D^+}(s_1, s)$ are multiplied by the small coupling constant $g_{D^{*+}\pi^+D^0}^2/(16\pi) \approx 0.00289$ GeV² which is small because $\Gamma_{D^{*+}}^{tot}(m_{D^{*+}}^2)$ is small. Numerical calculation shows that in the T_{cc}^+ resonance region, the contribution of the diagrams in Fig. 3 increases the width $\Gamma_{T_{cc}^+ \rightarrow D^{*+}D^0 \rightarrow \pi^+D^0D^0}(s_1)$ compared to its values in the tree approximation (see Fig. 2) by about 5%, 6%, 2%, and 0.6% at $\sqrt{s_1} = 3.874$ GeV, 3.875 GeV, 3.876 GeV, and 3.877 GeV, respectively. This is mainly due to the interference between the amplitudes of the loop diagrams in Fig. 3 and the amplitudes of the tree diagrams in Fig. 1. Of course, the real parts of the triangle loops play the main role in the interference. Note that integrations in Eq. (1) with substitutions Eqs. (3) and (4) smooth out sharp jumps in the functions $F_{D^{*+}D^0}(s_1, s)$ and $F_{D^{*0}D^+}(s_1, s)$. Taking into account the finite widths of the D^{*+} and D^{*0} mesons in their propagators entering into triangle loops also smoothes the logarithmic singularities and reduces the above estimates by approximately 10%. As for the Schmid theorem [30] about the modification of the tree contribution by the logarithmic singular imaginary part of the loop contribution (the modern analysis of this theorem is presented in Refs. [27, 31]), it holds in this case to the extent that it is permitted by the breaking of isotopic symmetry due to masses of the particles involving into the triangle loops $D^{*+}\pi^+D^0$ and $D^{*0}\pi^0D^+$ and also by the instability of D^* mesons.

Thus, we can conclude that the tree approximation for calculating the decay width $T_{cc}^+ \rightarrow (D^{*+}D^0 + D^{*0}D^+) \rightarrow \pi^+D^0D^0, \pi^0D^0D^+, \gamma D^0D^+$ used in Refs. [3, 4] is quite sufficient at the current level of measurement accuracy.

As regards spin effects, we note the following. From general considerations, spin effects in the essentially nonrelativistic decay $T_{cc}^+ \rightarrow D^{*+}D^0 \rightarrow \pi^+D^0D^0$ should not crucially change the assessment of the role of final state interactions. Here, the unchanging factors are the smallness of the width $\Gamma_{D^{*+} \rightarrow \pi^+D^0}(s = m_{D^{*+}}^2)$ and positions triangle singularities. The structure of the formulas that take into account the loop corrections will be generally similar to Eqs. (3) and (4). There are no special factors that would enhance the corrections (but the intermediate calculations become much more complicated). We hope to consider spin effects somewhere else.

ACKNOWLEDGMENTS

The work was carried out within the framework of the state contract of the Sobolev Institute of Mathematics, Project No. FWNF-2022-0021.

-
- [1] F. Muheim, Highlights from the LHCb Experiment, the European Physical Society Conference on High Energy Physics 2021, <https://indico.desy.de/event/28202/contributions/102717/>.
- [2] I. Polyakov, Recent LHCb results on exotic meson candidates, the European Physical Society Conference on High Energy Physics 2021, <https://indico.desy.de/event/28202/contributions/105627/>.
- [3] R. Aaij *et al.* (LHCb Collaboration), Observation of an exotic narrow doubly charmed tetraquark, arXiv:2109.01038.
- [4] R. Aaij *et al.* (LHCb Collaboration), Study of the doubly charmed tetraquark T_{cc}^+ , arXiv:2109.01056.
- [5] N. Li, Z. F. Sun, X. Liu, and S. L. Zhu, Perfect DD^* molecular prediction matching the T_{cc} observation at LHCb, *Chin. Phys. Lett.* **38**, 092001 (2021).
- [6] L. Meng, G. J. Wang, B. Wang, and S. L. Zhu, Probing the long-range structure of the T_{cc} with the strong and electromagnetic decays, *Phys. Rev. D* **104**, L051502 (2021).
- [7] A. Feijoo, W. H. Liang, and E. Oset, $D^0 D^0 \pi^+$ mass distribution in the production of the T_{cc} exotic state, *Phys. Rev. D* **104**, 114015 (2021).
- [8] Q. Qin, Y. F. Shen, and F. S. Yu, Discovery potentials of double-charm tetraquarks, *Chin. Phys. C* **45**, 103106 (2021).
- [9] M. Albaladejo, T_{cc}^+ coupled channel analysis and predictions, *Phys. Lett. B* **829**, 137052 (2022).
- [10] R. Chen, Q. Huang, X. Liu, and S. L. Zhu, Predicting another doubly charmed molecular resonance $T_{cc}^+(3876)$, *Phys. Rev. D* **104**, 114042 (2021).
- [11] M. J. Yan and M. P. Valderrama, Subleading contributions to the decay width of the T_{cc}^+ tetraquark, *Phys. Rev. D* **105**, 014007 (2022).
- [12] M. L. Du, V. Baru, X. K. Dong, A. Filin, F. K. Guo, C. Hanhart, A. Nefediev, J. Nieves, and Q. Wang, Coupled-channel approach to T_{cc}^+ including three-body effects, *Phys. Rev. D* **105**, 014024 (2022).
- [13] E. Braaten, L. P. He, K. Ingles, and J. Jiang, Triangle singularity in the production of $T_{cc}^+(3875)$ and a soft pion, arXiv:2202.03900.
- [14] J. He and X. Liu, The quasi-fission phenomenon of double charm T_{cc}^+ induced by nucleon, *Eur. Phys. J. C* **82**, 387 (2022).
- [15] X. Z. Ling, M. Z. Liu, L. S. Geng, E. Wang, and J. J. Xie, Can we understand the decay width of the T_{cc}^+ state?, *Phys. Lett. B* **826**, 136897 (2022).
- [16] M. Mikhasenko, Effective-range expansion of the T_{cc}^+ state at the complex $D^{*0} D^0$ threshold, arXiv:2203.04622.
- [17] L. Meng, B. Wang, G. J. Wang, and S. L. Zhu, Chiral perturbation theory for heavy hadrons and chiral effective field theory for heavy hadronic molecules, arXiv:2204.08716.
- [18] P. A. Zyla *et al.* (Particle Data Group), Review of particle physics, *Prog. Theor. Exp. Phys.* **2020**, 083C01 (2020) and 2021 update.
- [19] R. Omnès, On the solution of certain singular integral equations of quantum field theory, *Nuovo Cimento* **8**, 316 (1958).
- [20] Gabriel Barton, *Introduction to Dispersion Techniques in Field Theory* (W. A. Benjamin, Inc., New York, Amsterdam, 1965).
- [21] C. Roiesnel and T. N. Truong, Resolution of the $\eta \rightarrow 3\pi$ problem, *Nucl. Phys.* **B187**, 293 (1981).
- [22] D. J. Miller and D. R. Tovey, Kinematics, minireview in Ref. [18].
- [23] N. N. Achasov, S. A. Devyanin, and G. N. Shestakov, Is there a "signature" of the $\delta(980)$ meson four-quark nature?, *Phys. Lett.* **96B**, 168 (1980).
- [24] C. Fronsdal and R.E. Norton, Integral representations for vertex functions, *J. Math. Phys. (N.Y.)* **5**, 100 (1964).
- [25] M. Bayar, F. Aceti, F. K. Guo, and E. Oset, A discussion on triangle singularities in the $\Lambda_b \rightarrow J/\psi K^- p$ reaction, *Phys. Rev. D* **94**, 074039 (2016).
- [26] N. N. Achasov and G. N. Shestakov, Decay $X(3872) \rightarrow \pi^0 \pi^+ \pi^-$ and S -wave $D^0 \bar{D}^0 \rightarrow \pi^+ \pi^-$ scattering length, *Phys. Rev. D* **99**, 116023 (2019).
- [27] F. K. Guo, X. H. Liu, and S. Sakai, Threshold cusps and triangle singularities in hadronic reactions, *Prog. Part. Nucl. Phys.* **112**, 103757 (2020).
- [28] G. 't Hooft and M. Veltman, Scalar one-loop integrals, *Nucl. Phys. B* **153**, 365 (1979).
- [29] A. Denner, Techniques for the calculation of electroweak radiative corrections at the one-loop level and results for W physics at LEP200, *Fortschr. Phys.* **41**, 307 (1993).
- [30] C. Schmid, Final-state interactions and the simulation of resonances, *Phys. Rev.* **154**, 1363 (1967).
- [31] V. R. Debastiani, S. Sakai, and E. Oset, Considerations on the Schmid theorem for triangle singularities, *Eur. Phys. J. C* **79**, 69 (2019).